



Integration of a GIS and a complex three-dimensional hydrodynamic, sediment and heavy metal transport numerical model

Sandy M.Y. Ng^{a,*}, Onyx W.H. Wai^a, Yok-Shueng Li^a, Zhi-Lin Li^b, Yuwu Jiang^c

^a Department of Civil and Structural Engineering, The Hong Kong Polytechnic University, Hung Hom, Kowloon, Hong Kong SAR, China

^b Department of Land Surveying and Geo-Informatics, The Hong Kong Polytechnic University, Hung Hom, Kowloon, Hong Kong SAR, China

^c State Key Laboratory of Marine Environmental Science, Xiamen University, Xiamen, Fujian, China

ARTICLE INFO

Article history:

Received 30 August 2006

Received in revised form 18 July 2008

Accepted 16 September 2008

Available online 22 November 2008

Keywords:

Hydrodynamics

Sediment and heavy metal transport

Geographic information system

GIS-model integration

Three-dimensional visualization of coastal data

ABSTRACT

The paper presents an integration of a geographic information system (GIS) and a complex three-dimensional hydrodynamic sediment and heavy metal transport numerical model. The integration overcomes the two-dimensional constraint of conventional GIS by supplementing advance tools for three-dimensional, dynamic visualization. The application of a GIS-based interface module together with the three-dimensional, dynamic display tools enhances communication of relationships and trends of hydrodynamic and pollutant transport simulation in both spatial and temporal context, and thus promotes better coastal water quality planning and management. Model functionality includes input data viewing and editing, mesh grid configuration, and result interpretation. The functionality of the GIS-model integrated system is illustrated through a case study on the Pearl River Estuary (PRE).

© 2008 Elsevier Ltd. All rights reserved.

1. Introduction

The use of numerical models is the most feasible approach to solving hydrodynamic and pollutant transport problems. However, such complex models generally involve vast amounts of geographically-referenced information, and thus require enormous efforts in preparation of input data as well as in handling of output results for interpretation. Numerous efforts have been made over the decade to integrate hydrodynamic and pollutant transport models with geographic information system (GIS) [1–3]. Such integrations not only make efficient the modelling pre-processing and post-processing procedures, but also provide the system with spatial data management, analysis, and visualization functionalities.

Although GIS is demonstrated to be an invaluable asset in hydrodynamic and pollutant transport modelling, there is one major constraint in its implementation. Marine environmental data exhibit variations not only in both location and depth, but also through time [4]. It is difficult to establish a rigorous model to represent the ever-changing, three-dimensional nature of marine system in a GIS environment. This explains why most of the current GIS-hydrodynamic/pollutant transport models are limited to two-dimensional capabilities. Since hydrodynamics is intrinsically three-dimensional and dynamic, such models oversimplify the real

situations and generate results with limited accuracy. As the fundamental concept of GIS is mapping of information in two-dimensional ground, there is a considerable challenge in unfolding this two dimensionality for applications into the three and four-dimensional world.

This paper describes the integration of a GIS and a complex three-dimensional hydrodynamic sediment and heavy metal transport numerical model. The model was developed at The Hong Kong Polytechnic University [5] to tackle the deteriorating water quality conditions at the Pearl River Estuary (PRE). The model covers the prediction of hydrodynamic patterns and sediment and heavy metal transports for the entire PRE using the finite element method. Such complex computation requires the model to be run on an efficient parallel computing system of ten CPUs using Message Passing Interface (MPI) scripting.

The parallelized system is implemented using a LINUX operating system, in which its user-friendliness is incomparably lower than that of proprietary operating systems such as Windows or MacOS. Both model input and output involve a substantial quantity of spatial data, however, the model is not equipped with any tools to handle spatial analysis and visualization. This constraint marks the necessity to provide the essential graphical tools for preparations and displays of model inputs and outputs; and the integration of the model with a GIS is identified as a plausible approach.

The primary objective of the integration is to build a connection between the model and a GIS. Using input data created in the GIS,

* Corresponding author. Tel.: +852 6278 0864; fax: +852 2334 6389.

E-mail address: samanyi24@hotmail.com (S.M.Y. Ng).

numerical simulations can be run and model results can be analyzed in the GIS. Furthermore, to overcome the two-dimensional limitation of conventional GIS, a set of data displaying tools are developed to offer interpretation of information in the third (i.e. depth) and fourth (i.e. time) dimensions.

2. A complex, three-dimensional hydrodynamic sediment and heavy transport numerical model

In this study, a GIS is integrated with a complex, three-dimensional hydrodynamic sediment and heavy transport numerical model. This model was initially developed by Wai and Lu [6] with the key purpose to simulate hydrodynamic and sediment transport processes in coastal and estuarine regions using an efficient parallel-processing algorithm. The information derived from the model is essential for design and management of coastal infrastructure as well as for monitoring of water quality and wastewater discharge. The model was later improved by Jiang [7] to include the fate and transport of cohesive sediment and heavy metals modelling. Jiang [7] also adopted more advanced algorithms, including parallelized Eulerian–Lagrangian operator splitting strategy for solving large linear equation system, the level 2.5 turbulence closure sub-model to improve the accuracy of the vertical eddy viscosity coefficient estimation, and the finite element method for solving vertical diffusion term, and successfully applied it for simulating the PRE situation.

The model is made of a set of sub-components as shown in Fig. 1. The hydrodynamic model together with the turbulence and salinity modules forms the base model. Variables are passed through two auxiliary models for predictions of cohesive sediment and heavy metal concentrations.

2.1. Base model

The base model is built upon the Navier–Stokes equations with the assumption that hydrodynamics in estuaries and coasts is isothermal; and the vertical acceleration is negligible in comparison with gravitational acceleration, resulting in hydrostatic pressure distribution. In the hydrodynamic module, important phenomena including turbulence and salinity are also considered. The governing equations are given as follows:

Continuity equation:

$$\frac{\partial \zeta}{\partial t} + \frac{\partial H u_j}{\partial x_j} = 0 \tag{1}$$

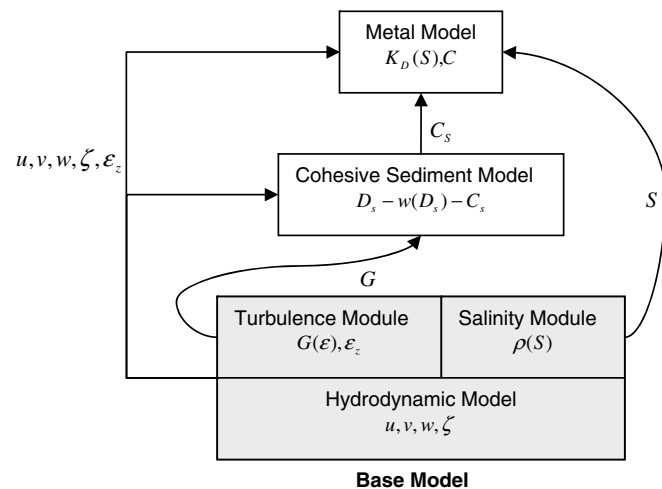


Fig. 1. Computation flow of the complex, three-dimensional hydrodynamic sediment and heavy transport numerical model [7].

Momentum equation (Navier–Stokes equations):

$$\frac{du_i}{dt} + f\beta_{ij}u_j + P_i^* + g\frac{\partial \zeta}{\partial x_i} = \frac{\partial}{\partial x_j} \left(\epsilon_{ij} \frac{u_i}{x_j} \right) \tag{2}$$

Salinity transport equation:

$$\frac{\partial S}{\partial t} = \frac{\partial}{\partial x_j} \left(\epsilon_{sali,j} \frac{S}{x_j} \right) \tag{3}$$

Level 2.5 turbulence closure model:

$$\frac{\partial q^2}{\partial t} = \frac{\partial}{\partial x_j} \left(\epsilon_{q,j} \frac{q^2}{x_j} \right) + \frac{2\epsilon_{q,z}}{H^2} \left(\frac{\partial u_i}{\partial \sigma} \right)^2 + \frac{2g\epsilon_{sali,z}}{\rho_0 H} \frac{\partial \rho}{\partial \sigma} - \frac{2q^3}{B_1} \tag{4}$$

$$\begin{aligned} \frac{\partial q^2 l}{\partial t} = & \frac{\partial}{\partial x_j} \left(\epsilon_{q,j} \frac{q^2 l}{x_j} \right) + \frac{E_1 l \epsilon_z}{H^2} \left(\frac{\partial u_i}{\partial \sigma} \right)^2 + E_1 E_3 l \frac{g \epsilon_{sali,z}}{\rho_0 H} \frac{\partial \bar{\rho}}{\partial \sigma} \\ & - (1 + E(l/kL)^2) \frac{q^3}{B_1} \end{aligned} \tag{5}$$

where $u_j = \{u, v, \omega\}$, $\omega = \frac{1}{H} [w + (1 - x_3)u_i \frac{\partial h}{\partial x_i} - x_3 (\frac{\partial \zeta}{\partial t} + u_i \frac{\partial \zeta}{\partial x_i})]$; $\epsilon = [\epsilon_x, \epsilon_y, \epsilon_z H^{-2}]$; $\epsilon_{sali,j} = [\epsilon_{sali,x}, \epsilon_{sali,y}, \epsilon_{sali,z} H^{-2}]$; $x_j = [x, y, (z + h)H^{-1}]$; $H = h + \zeta$; $\beta_{ij} = \begin{bmatrix} 0 & -1 & 0 \\ 1 & 0 & 0 \end{bmatrix}$; $i = 1, 2, 3$; $j = 1, 2, 3$; $\epsilon_{q,j} = [\epsilon_{q,x}, \epsilon_{q,y}, \epsilon_{q,z} H^{-2}]$; $L = [(\eta - z)^{-1} + (H - z)^{-1}]^{-1}$; $\frac{\partial \bar{\rho}}{\partial \sigma} \equiv \frac{\partial \rho}{\partial \sigma} - \frac{1}{v_s^2} \frac{\partial \rho}{\partial \sigma}$; where t is time; h is the water depth relative to the minimum water level; ζ is the water surface elevation relative to the minimum water level; x_1, x_2, x_3 are the spatial coordinates in sigma σ coordinates; u, v, ω are velocity components along the x, y, z -directions, respectively, in σ coordinates; w is the vertical velocity in Cartesian coordinate; $\epsilon_x, \epsilon_y, \epsilon_z$ are the eddy viscosity coefficients for water in the x, y, z -directions, respectively; $\epsilon_{sali,x}, \epsilon_{sali,y}, \epsilon_{sali,z}$ are the eddy diffusion coefficients for salinity in the x, y, z -directions, respectively; g is the gravity acceleration; f is the Coriolis coefficient; S is the water salinity; ρ is the water density; ρ_0 is the constant reference water density; $q^2/2$ is the turbulence energy; l is the master turbulence length scale; $\epsilon_{q,x}, \epsilon_{q,y}, \epsilon_{q,z}$ are the eddy diffusion coefficients for turbulence energy in the x, y, z -directions, respectively; p is the water pressure; v_s is the speed of sound; the constant coefficients are $E_1 = 1.8, E_2 = 1.33, E_3 = 1.0, B_1 = 0.74$ and $k = 0.4$, and P_i^* is the baroclinic term with Boussinesq assumption in the x_i direction given by the following equation:

$$P_i^* = \frac{gH}{\rho} \int_{\sigma}^1 \frac{\partial \rho}{\partial x_i} d\sigma - \frac{g}{\rho} \frac{\partial H}{\partial x} \int_{\sigma}^1 (\sigma - 1) \frac{\partial}{\partial \sigma} d\sigma \tag{6}$$

The water density ρ is a function of temperature T and chlorinity Cl :

$$\rho = 1000 + 1.455Cl - 0.0065(T - 4 + 0.4Cl)^2 \tag{7}$$

and Cl relates to salinity by

$$Cl = (S - 0.03)/1.805 \tag{8}$$

The Smagorinsky formula is used to obtain the horizontal viscosity and coefficients, ϵ_i and $\epsilon_{sali,i}$

$$\epsilon_i, \epsilon_{sali,i} = \frac{1}{2} CA \left[\left(\frac{\partial u_1}{\partial x_1} \right)^2 + \frac{1}{2} \left(\frac{\partial u_1}{\partial x_2} + \frac{\partial u_2}{\partial x_1} \right)^2 + \left(\frac{\partial u_2}{\partial x_2} \right)^2 \right]^{1/2} \tag{9}$$

where C is a constant ranging from 0.1 to 0.2, A is the area of the triangular elements. The Level 2.5 turbulence closure model adopted by Mellor–Yamada [8] is applied for computation of vertical eddy viscosity and diffusion coefficients.

2.2. Cohesive sediment transport model

The fate of cohesive sediment is heavily influenced by flocculation as the floc settling velocity can be several orders of magnitude greater than that of primary particles. In this model, the floc size equation is coupled with the sediment concentration equation

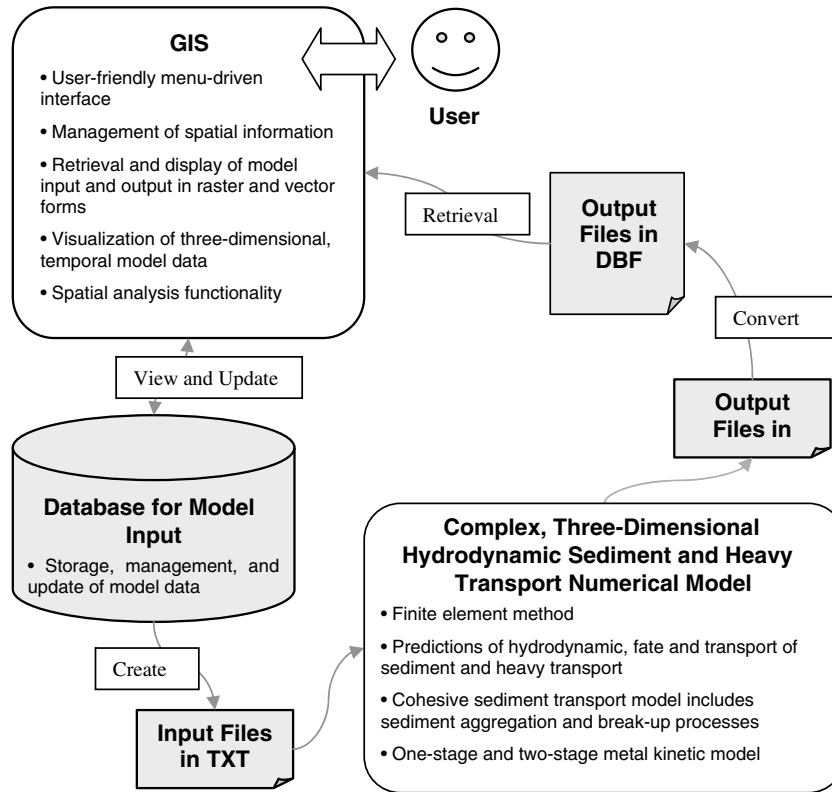


Fig. 2. Conceptual diagram of integration of a GIS and a complex three-dimensional hydrodynamic sediment and heavy metal transport numerical model.

for computation of the transport and fate of cohesive suspended sediments.

Sediment concentration equation:

$$\frac{\partial C_s}{\partial t} - \frac{\partial w_s C_s}{H \partial x_3} = \frac{\partial}{\partial x_j} \left(\varepsilon_{sed,j} \frac{C_s}{x_j} \right) \quad (10)$$

Floc size transport equation:

$$\frac{\partial D_s}{\partial t} - w_s \frac{\partial D_s}{H \partial x_3} = \frac{\partial}{\partial x_j} \left(\varepsilon_{sed,j} \frac{D_s}{x_j} \right) + K_A C_s G D_s^2 - K_B G^{3/2} D_s^2 (D_s - D_p) \quad (11)$$

where $\varepsilon_{sed,j} = [\varepsilon_{sed,x}, \varepsilon_{sed,y}, \varepsilon_{sed,z} H^{-2}]$; C_s is the cohesive sediment concentration; w_s is the apparent sediment settling velocity; $\varepsilon_{sed,x}, \varepsilon_{sed,y}, \varepsilon_{sed,z}$ are the eddy diffusion coefficients for sediment in the x, y, z -directions, respectively; D_s is the diameter of floc; K_A and K_B are break-up parameter; D_p is the diameter of primary particles; and G is the turbulence shear stress. The turbulence shear stress G is calculated by substituting the turbulence energy equation according to Mellor and Yamada [8]:

$$G = \sqrt{\frac{\varepsilon}{\nu}} = \sqrt{\frac{q^3}{Bl\nu}} \quad (12)$$

where ε is the turbulence energy dissipation rate; ν is the kinetics viscosity; and B is a constant set to 16.6.

2.3. Heavy metal transport model

The computation of the fate and transport of heavy metal is based on the one-stage and two-stage adsorption and desorption mechanism. The one-stage equation assumes the concentration of metal remains constant as the dissolved metal is adsorbed onto surface of sediment. The equations for the two-stage mechanism is adopted based on the theory by Jannasch et al. [9], which assumes

that the dissolved metal particle is adsorbed “quickly” onto the surface of sediment, and then deposit “slowly” into the inner part of sediment.

One-stage model:

Adsorbed metal concentration equation:

$$\frac{dP}{dt} = k(K_D C_d - P) + w_s \frac{\partial P}{\partial z} + \frac{\partial}{\partial x_j} \left(\varepsilon_{p,j} \frac{\partial P}{\partial x_j} \right) \quad (13)$$

Dissolved metal concentration equation:

$$\frac{dC_d}{dt} = -C_s k(K_D C_d - P) + \frac{\partial}{\partial x_j} \left(\varepsilon_{m,j} \frac{\partial C_d}{\partial x_j} \right) \quad (14)$$

Two-stage model:

First stage (fast process) metal sorption equation:

$$\frac{dP_1}{dt} = k(K_{D,1} C_d - P_1) - k_2(K_{D,2} P_1 - P_2) + w_s \frac{\partial P_1}{\partial x_3} + \frac{\partial}{\partial x_j} \left(\varepsilon_{p,j} \frac{\partial P_1}{\partial x_j} \right) \quad (15)$$

Second stage (slow process) metal sorption equation:

$$\frac{dP_2}{dt} = k_2(K_{D,2} P_1 - P_2) + w_s \frac{\partial P_2}{\partial x_3} + \frac{\partial}{\partial x_j} \left(\varepsilon_{p,j} \frac{\partial P_2}{\partial x_j} \right) \quad (16)$$

Dissolved metal concentration equation:

$$\frac{dC_d}{dt} = -C_s k_1(K_{D,1} C_d - P_1) + \frac{\partial}{\partial x_j} \left(\varepsilon_{m,j} \frac{\partial C_d}{\partial x_j} \right) \quad (17)$$

$$P = P_1 + P_2, \quad j = 1, 2, 3 \quad (18)$$

where P is the adsorbed/particulate metal concentration in $\mu\text{g/g}$; K_D is the partition coefficient in l/g ; k is the forward or reverse transfer rate in $1/s$; w_s is the particle setting velocity; $\varepsilon_{p,j} =$

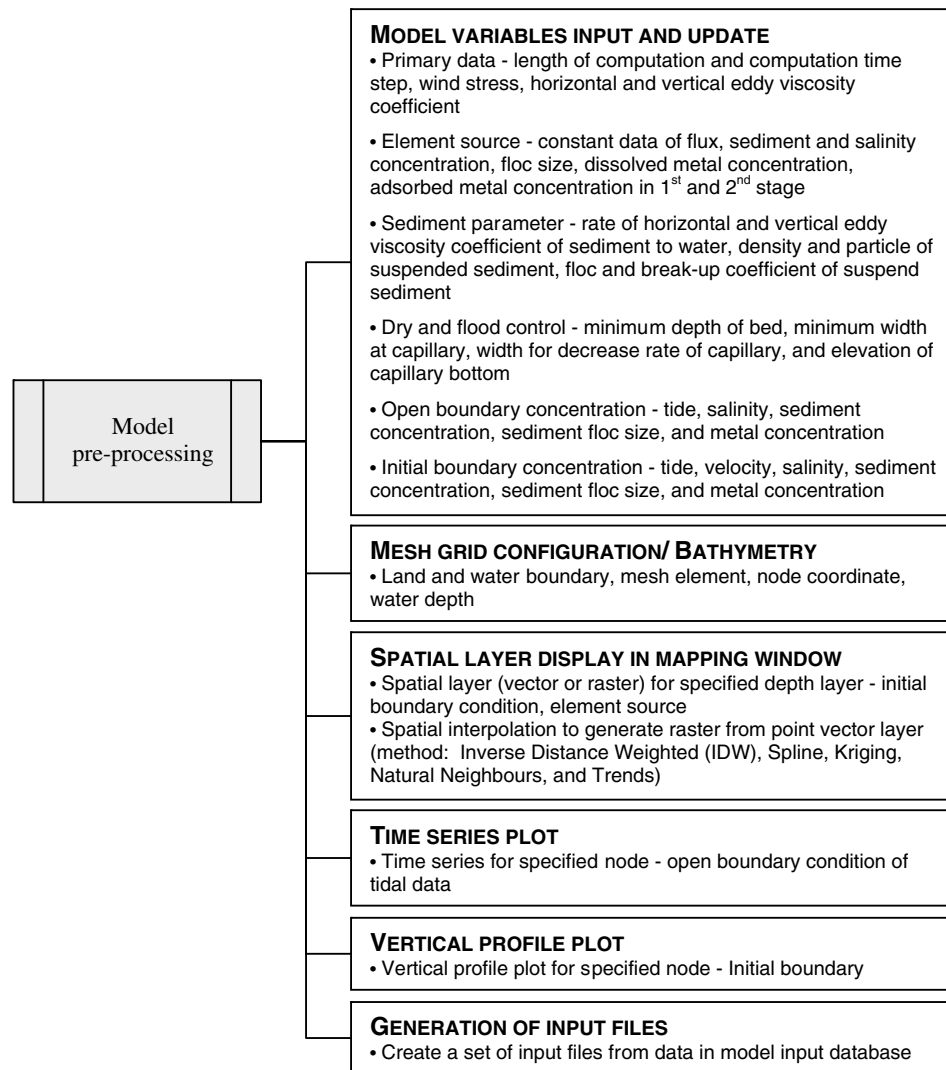


Fig. 3. Model pre-processing operations.

$[\epsilon_{p,x}, \epsilon_{p,y}, \epsilon_{p,zH^{-2}}]$, $\epsilon_{p,x}, \epsilon_{p,y}, \epsilon_{p,zH^{-2}}$ are the eddy diffusion coefficients for adsorbed/ particulate metal; C_d is the dissolved sediment concentration; C_s is the suspended sediment concentration; $\epsilon_{m,j}$ is the dissolved metal diffusivity coefficient in the j direction. The subscript "1" denotes the parameter of the first equilibrium partition at the sediment surface, where "2" denotes the interactive process in the inner sediment.

2.4. Modelling variables

The three-dimensional hydrodynamic sediment and heavy transport numerical model as described encompasses numerous direct and indirect variables. Direct variables include horizontal and vertical velocities, turbulence energy, bed shear stress, vertical viscosity, turbulence energy multiplied by characteristic length, sediment transport variables such as sediment concentration, sediment floc size, as well as other modelling concentrations such as salinity and metal concentration dissolved in water, metal concentration adsorbed on particle surface, and metal concentration adsorbed in inter particle. Indirect variables include the forcing inputs such as tidal level, concentrations prescribed at the boundaries, and so forth. All modelling variables are temporally-varying, while most are spatially-varying in three dimensions. This emphasizes the needs of a robust system for management and visualiza-

tion of the substantial quantity of temporal and spatial information.

3. Integration with a GIS

The development of the GIS-model integrated system is carried out using GIS Software ARCVIEW Version 9, developed by the Environmental Systems Research Institute, Inc. (ESRI). The software is customized using ARCVIEW's built-in Visual Basic for Application (VBA) scripting through the manipulation of ArcObjects. Advance data display tools are also developed from Active Dynamic Link Library (DLL) in Visual Basic (VB), and registered into the GIS. A user-friendly menu-driven interface is used to conduct GIS-related hydrodynamic analysis.

Fig. 2 shows a conceptual diagram of the GIS-model integrated system. The integration is implemented using a mid-level coupling method (i.e. interface integration method according to Shamsi [10]), enabling model pre-processing and pro-processing procedures to be completely carried out within the GIS menu-driven graphic user interface. Two separate flows of information are established between the GIS and the model, one for data input and the other for model output. This enables the user to update and view model input, modify mesh grid configuration, and retrieve and display model output through the GIS window. Basic

functionality of the GIS can also be applied for analysis of model results.

The integration using a mid-level coupling method allows full coverage of the model operations within the GIS interface, except for model execution. The reason for not extending the integration further for a tightly-coupled system lies upon the model operational scheme and the requirement of GIS capabilities for the model. The procedural implementation of the model consists of three sequential steps: (1) preparation of input file, (2) execution of model, and (3) retrieval of result from output. Note that the model does not provide any real-time generation of results, that is, results are outputted in a batch after model simulation is fully complete. The actual execution of the model is a single, distinct procedure that does not require any GIS capabilities. So the application of a mid-level coupling method is sufficient to meet the goal of integration, that is, to allow pre-processing and post-processing procedures to be carried out entirely within the GIS interface, for this study.

3.1. Model pre-processing

The data input requirements of the model include bathymetry of the study area, inflow and outflow for source elements, suspended and bed sediment parameters, tidal flat drying and flooding control variables, initial conditions and boundary conditions of tidal elevation, salinity, current velocity, sediment concentration, and metal concentration, as well as mesh grid configuration. The pre-processing component is developed for retrieval, manipulation, editing, display, and export of model input data through the GIS interface (see Fig. 3).

3.1.1. Data retrieval and update

All model inputs are primarily stored in forms of text file. A relational database is developed using the MS Access software for storage of model input (refer to Fig. 2). The placement of model input into a relational database serves two main purposes. The first is to allow efficient management and query of model input, and the second is to establish a direct linkage between the model input and the GIS user interface using Object Linking and Embedding (OLE) technology. Programming routines have been developed to allow retrieval and update of the input data tables through the input dialog boxes. Fig. 4 shows the dialog box for retrieval and editing of initial conditions of velocity. Similar data operation dialog boxes

are implemented for all other model inputs. An update files function is also incorporated into the software in order to complete the entire pre-processing implementation. The function takes the data from the database and creates input text files based on the data.

3.1.2. Data display

The pre-processing component also includes functions for graphic display of input data. There are three basic ways to display model input. The first method is a spatial layer (vector or raster) at a specified water depth layer through the GIS mapping window. The types of model input which can make practical use of spatial layer display are initial boundary conditions, water depths, as well as element source (i.e. concentration of pollutants released at river mouth or any other sources). A spatial layer can be created simply by specifying the parameter and the layer (not applicable for water depths and tidal data). Based on the selection criteria, the GIS performs SQL queries to extract the information from the model input data and displays in forms of point feature layers.

The values for model input parameters are attributed to node and layer numbers. In order to display the information spatially in form of a point feature layer, each nodal point is referenced to a geographic coordinate. The node geographic coordinates are all stored in a node coordinate table, which are connected with the other tables, for geographical reference during the system querying process. Fig. 5 shows the relational structure (i.e. one-to-many) between the node coordinate table and the tables for initial conditions and water depths.

The incorporation of spatial layer displays allows for quick and easy interpretation of information. Fig. 6 is a single spatial point layer of water depth created using the model input display command. The colour of the nodal points gradates from light to dark as the water depth varies from shallow to deep. Hence, the user can acquire, at a glance, a comprehensive picture of specified modal input variables. The spatial layer display function can also be implemented in a batch mode (i.e. more than one spatial layer can be created upon a single execution of command) to generate a block of profile spatial layer.

Two other data displaying functions, the time series and vertical profile plots, are also incorporated into the system for examining temporal and depth variation. Time series plot is only applicable for open boundary conditions of tidal level (as all other variables, such as sediment concentration, salinity, and metal concentration are assumed to be constant with time), while vertical profile display is for both initial and boundary conditions of all variables except tidal level and water depth.

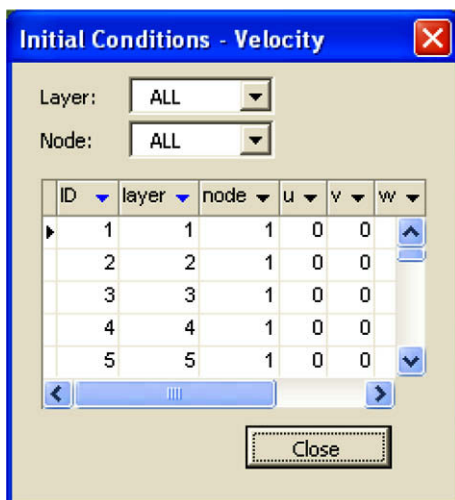


Fig. 4. Model input operation dialog box – initial conditions of velocity.

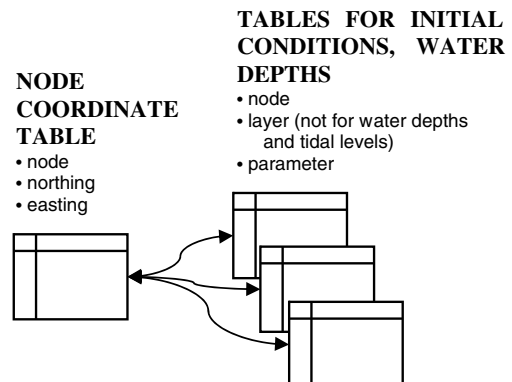


Fig. 5. Database relationship diagram – model input data.

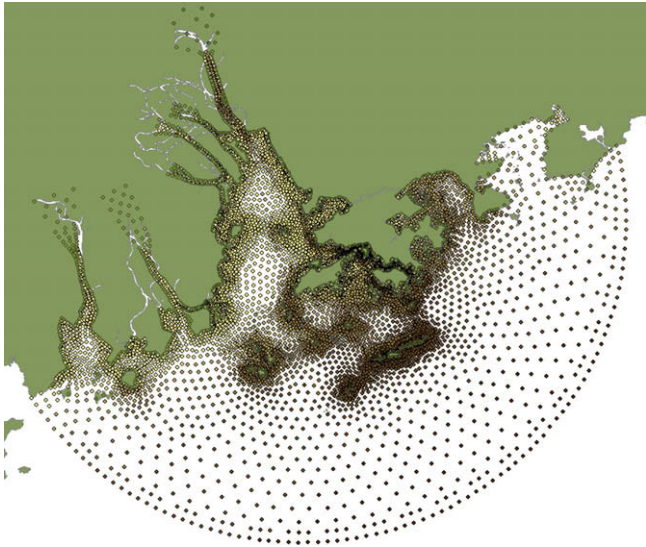


Fig. 6. Display of a spatial point layer of water depth from model input in the GIS mapping window.

3.1.3. Mesh grid configuration and refinement

Mesh grid configuration is another important procedure which makes efficient use of GIS through the integration. The mesh grid of this model is composed of a set of triangular elements, and each triangular element is configured based on a set of six nodal points, three for corner points and three for middle points. A set of modules is developed for generating the mesh grid through the GIS interface as well as for editing the grid elements.

The setup of the mesh grid is derived primarily from two input tables, one identifies the six nodal numbers for each triangular element and the other provides the coordinates of nodal points. Fig. 7 shows the dialog box for viewing the mesh grid configuration in numeric format. To allow spatial examination of the mesh in the mapping window, programming routine is written for generating shapefiles resembling the mesh grid configuration based on data

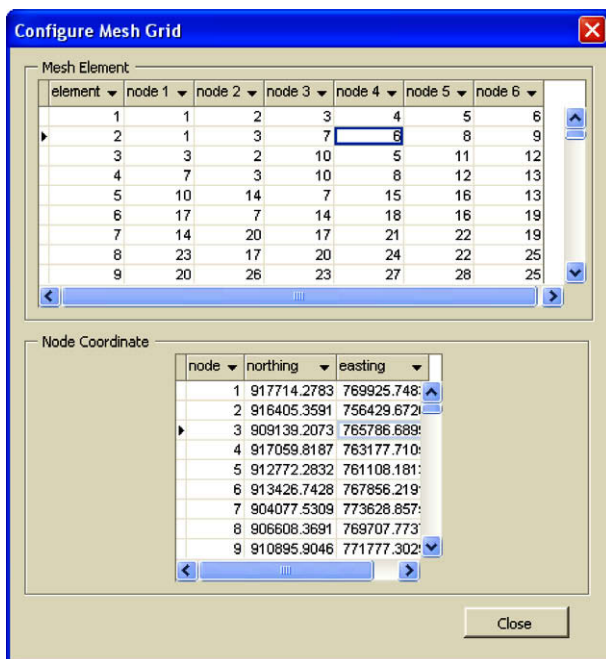


Fig. 7. Dialog box for configuring mesh grid.

from these two input tables. The mesh grid generation function creates three shapefiles: one polygon shapefile representing the triangular elements, one point shapefile for all nodes, and another point shapefile for the corner nodes only. Fig. 8 shows the generated mesh grid in the GIS mapping window.

In addition, a mesh grid edit toolbar is also incorporated into the system which allows the user to refine the mesh grid by moving the nodes using the cursor in the GIS mapping window. The arrangement of the triangular element relies merely on the corner nodes. Upon initialization of the mesh grid edit session, the GIS turns off (i.e. make invisible) the shapefile for all nodal points in order to reinforce that only the shapefiles for mesh element and corner points are allowed for selection and editing. The user can re-configure the mesh grid by moving the corner nodes and the program keeps track which corner node has been modified. At termination of the edit session, the system carries out two types of update, one for the coordinate tables in the model input database and the other for the shapefiles. Since geometrically a middle node must lie halfway between the two corner nodes, the coordinate for each middle node can be calculated simply by taking the average of the coordinates for the two corner nodes. Based on the new coordinate values for middle and corner nodes, the system updates both the coordinate table and the three shapefiles.

3.2. Model post-processing

The main intention of the post-processing component is to take the model output data and display them in forms of spatial layer (vector or raster), time series, and profile (see Fig. 9). Same as the model input, the model output consists of a set of text files. A module is written to convert the output text file into Database File (DBF) format (refer to Fig. 2). The retrieval data in DBF format rather than in text format improves the system efficiency.

The model output variables include sediment concentration, sediment floc size, salinity, metal concentration dissolved in water, metal concentration adsorbed on particle surface, metal concentration adsorbed in inter particle, tidal level, depth from sea mean level, horizontal velocity magnitude and direction, vertical velocity magnitude, horizontal viscosity by Smagorinsky formula, vertical viscosity by turbulence module for water, vertical viscosity by turbulence module for salinity, vertical viscosity by turbulence module for turbulence, turbulence energy, turbulence energy

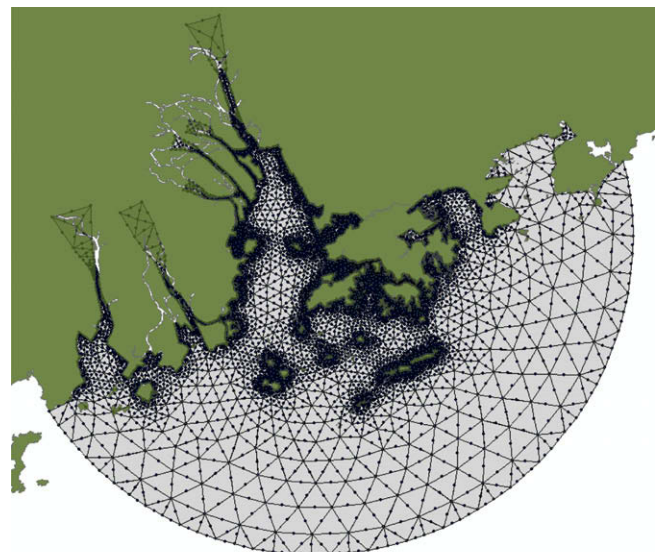


Fig. 8. The Pearl River Estuary: finite element mesh.

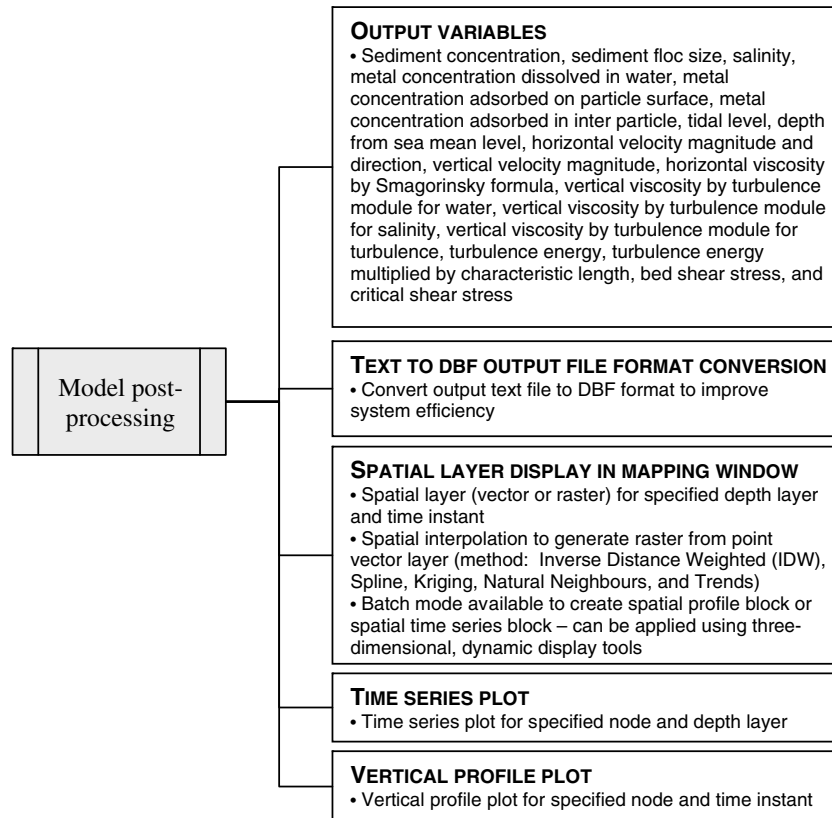


Fig. 9. Model post-processing operations.

multiplied by characteristic length, bed shear stress, and critical shear stress. All variables, except for tidal level, are referenced by three spatial coordinates and a temporal coordinate. Thus, the spatial layer of a typical variable is retrieved from the input of the water depth layer and the simulation time (see Fig. 10). A number of spatial interpolation methods – Inverse Distance Weighted (IDW), Spline, Kriging, Natural Neighbours, and Trends – can be applied to create raster layers from the retrieved point feature layers. A time series is retrieved from input of the water depth layer and nodal number, while a profile plot is generated from input of nodal number and simulation time.

Spatial layers can also be retrieved in a batch mode such that all layers from the same time instant or the same water depth layer are created using a single command. The result is a spatial profile block or a spatial time series block. Furthermore, the spatial profile block for several time instants can be generated at once, resulting in a temporal set of spatial profile blocks (see Fig. 11). The next section discusses three interactive toolbars for three-dimensional, dynamic visualization used in conjunction with the spatial profile

raster block, the spatial time series raster block, and the temporal set of spatial profile raster blocks.

3.3. Three-dimensional, dynamic display tools

Three interactive toolbars are developed for three-dimensional, dynamic display of the model result. These include profile and section display, time series dynamic display, and dynamic section display.

3.3.1. Profile and section display

The profile and section display toolbar is implemented with a spatial profile raster block, which is consisted of a set of spatial raster layers taken at different depth layer at the same time instant. Both operations of the profile and section displays require first specifying the name of the spatial profile raster block. For the profile display, the user can then click any point within the map region. A programming routine has been written, which extracts value at the selected point from each of the raster layers in the profile block, and generates a profile plot using the extracted values (see Fig. 12).

Similar data extraction technique is applied in developing the section plot display tool. However, instead of selecting a single point in the map region, the user needs to click two points to specify a line. Upon execution, the system first derives the bathymetry along the line from a raster depth layer for creating a polygon object representing the seabed. Then, from each raster layer, several discrete values are taken along the specified line and plotted onto a point feature shapefile for section. Spatial interpolation is further applied to convert the point feature shapefile into a raster layer. The final step is the overlay of the seabed polygon object onto the rectangular raster image, resulting in a colormap resembling the sectional view of the specified parameters (see Fig. 13).

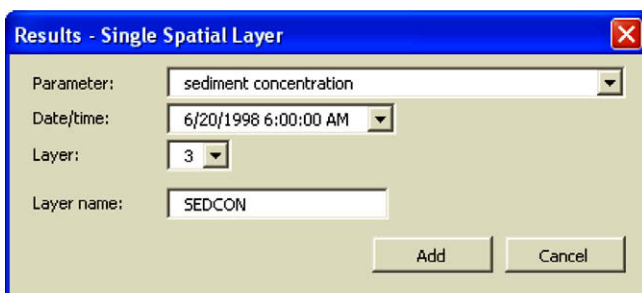


Fig. 10. Model output operation dialog box – a single spatial layer.

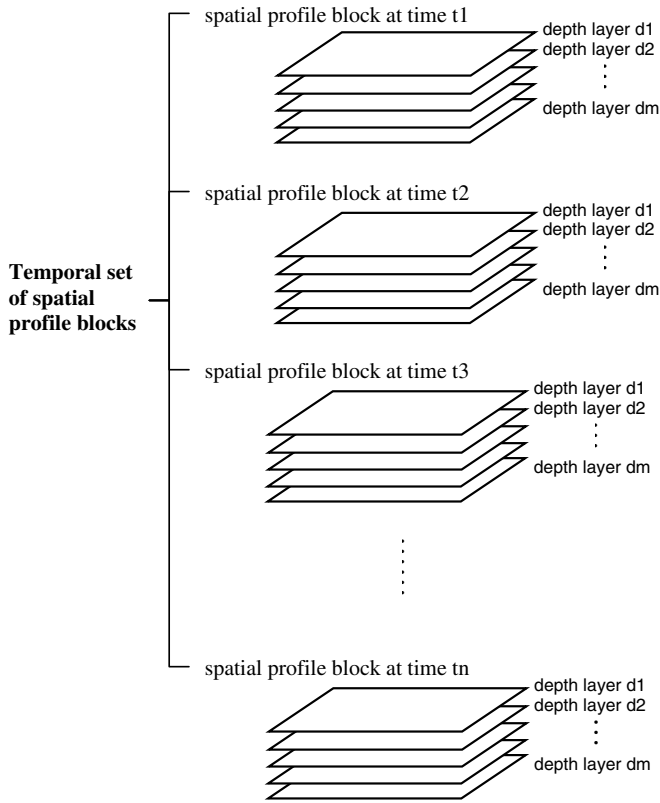


Fig. 11. Temporal set of spatial profile blocks.

3.3.2. Time series dynamic display

As hydrodynamic marine environment is continuously changing, dynamic display is an essential tool for examining and analyzing temporal variation of coastal data. The time series dynamic display follows the same data extraction concept as the profile display. Values at a specified point are extracted from each layer of a specified spatial time series raster block to generate a time series curve. A module for dynamic display of the spatial layers is developed using the VB Timer control. The animated temporal variation of a specified parameter is generated by adjusting the visibility of raster layers within the spatial time series raster block over time. For instance, layer 1 is visible only at time t1, layer 2 is visible only at time t2, and so on. In addition, a cursor moves dynamically along the time series curve to the position (i.e. time) corresponding to that of the visible layer (see Fig. 14). Additional features are playback controls such as pause, stop buttons, and play speed adjustment.

3.3.3. Dynamic section

The development of the dynamic section is derived from the programming techniques used in the section display and the time series dynamic display tools. The dynamic section is implemented by first specifying the temporal set of spatial profile blocks, and then selecting a two points on the mapping window to create a line along which the dynamic section is created. The system then applies the same data extraction and interpolation techniques for creating section raster layer for each of the spatial profile block in the temporal set. The execution of dynamic section is carried out by adjusting the visibility of the section raster layers.

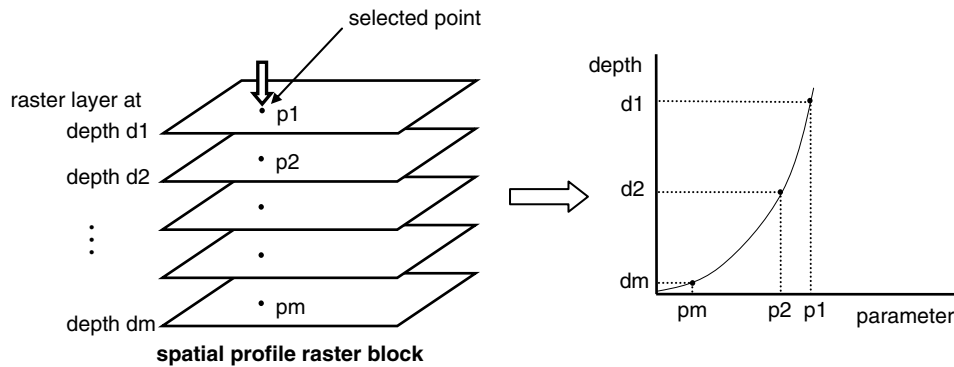


Fig. 12. Profile plot display tool.

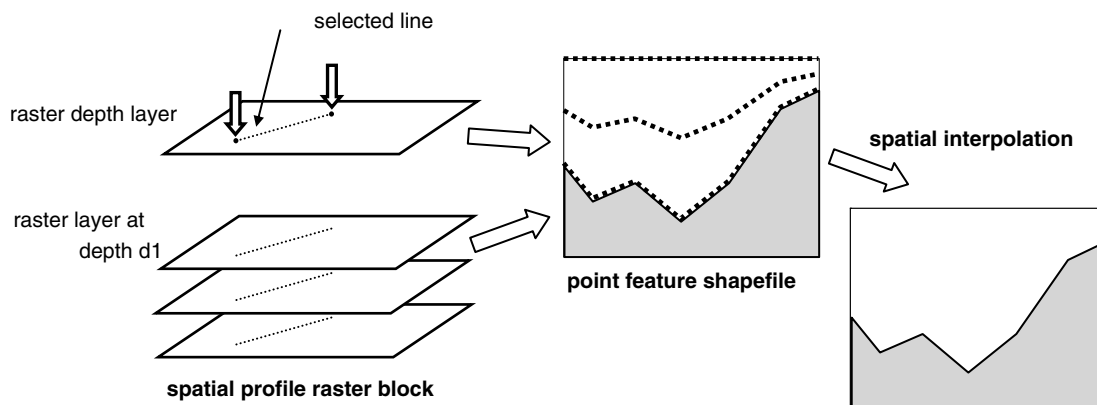


Fig. 13. Section plot display tool.

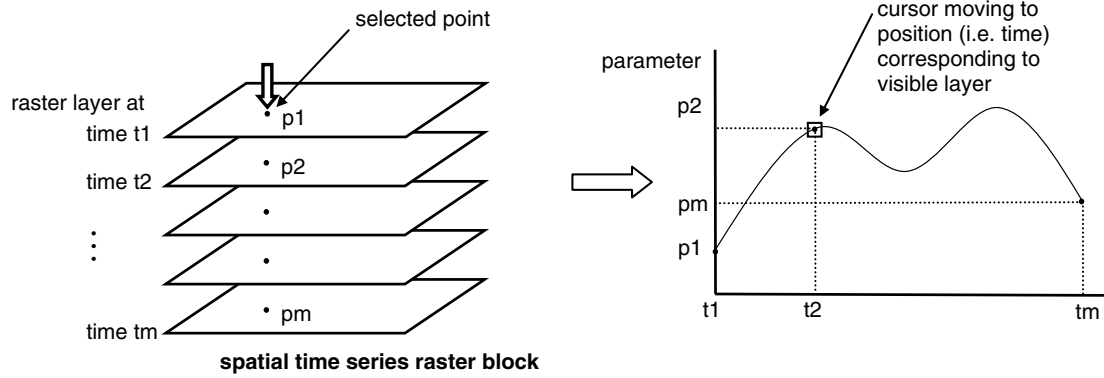


Fig. 14. Time series display tool.

4. Case study

An application for the PRE is presented to illustrate the functionality of the GIS-model integrated system. The PRE is a 2000 km² triangular-shaped estuary located at the southern part of China. The estuary receives freshwater from four major river outlets, namely, Humen, Jiaomen, Hongqilimen, Hengmen and drains into the South China Sea. The rapidly growing economic industrial development in the recent decades in the Pearl River Delta (PRD) have lead to severe degradation of water quality in the PRE system.

Fig. 15 provides a comprehensive overview on the model input setup of the simulation, including water depth raster layer, element sources, mesh grid configuration and boundary conditions of tidal elevation. The water depth raster layer is generated from interpolation of the model input bathymetry point data. The water depth ranges from 0 to 72 m. The *Identify Results* dialog box shows the information at element source number 1855. The inflows of element source include flux, sediment concentration, salinity, floc size, dissolved metal, and adsorbed metal at first and second stage. The time series display shows the tidal elevations at boundary node number 23. The model simulation was carried out for a one-week wet season period from June 21 to 28, 1998.

A set of model input text files were generated following the update of model input. Model simulation was then carried out using the model input text files. An initial “warm up” run was first undertaken to establish steady state flow condition. Once steady state flow condition was reached, element source concentrations were then introduced into the system. The “warm up” run took only about 20 min and the entire model simulation was approximately three hours. The model generated a set of model output text files after the simulation is complete. The model output text files were further converted to DBF files for efficient retrieval.

Fig. 16 shows the model mesh grid displayed in the GIS mapping window with a node (i.e. node number 1880) highlighted in red, from which the tidal level is generated. June 24, 1998 12:00:00 pm corresponds to the time of ebbing tide at node number 1880. A point spatial layer of current velocity overlaying a raster of salinity for the surface layer is generated at this simulation time as shown in Fig. 17. It can be seen that the direction of the current corresponds well with the ebbing tide. The current is moving away from the coastal region towards the sea. The salinity is represented by a graduated colour scale, with the lightest shade for the lowest value (i.e. 0 ppt) and the darkest shade for the highest value (i.e. 35 ppt). The salinity is relatively low at the shore area and increases gradually towards the open sea.

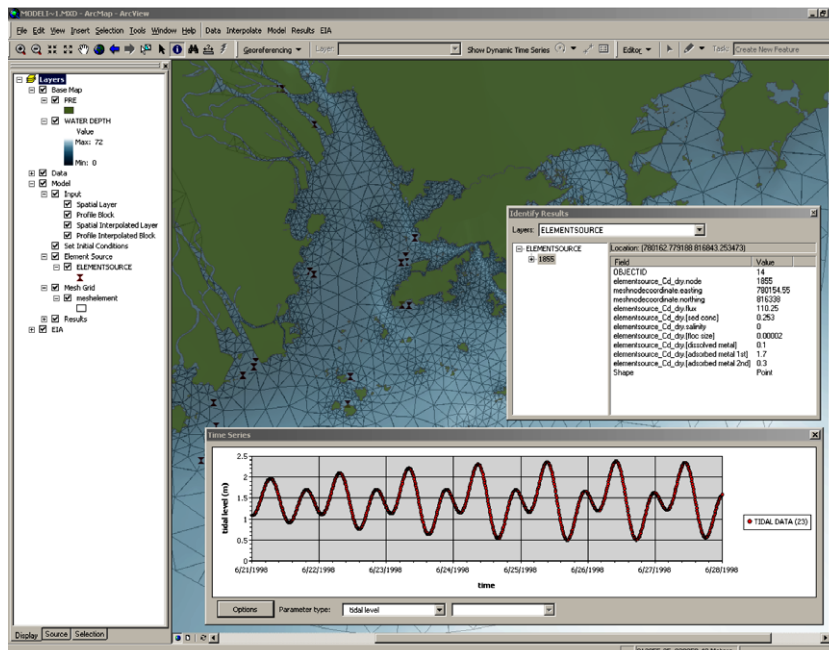


Fig. 15. Display of model input of element source and tidal level using the GIS-model integrated system.

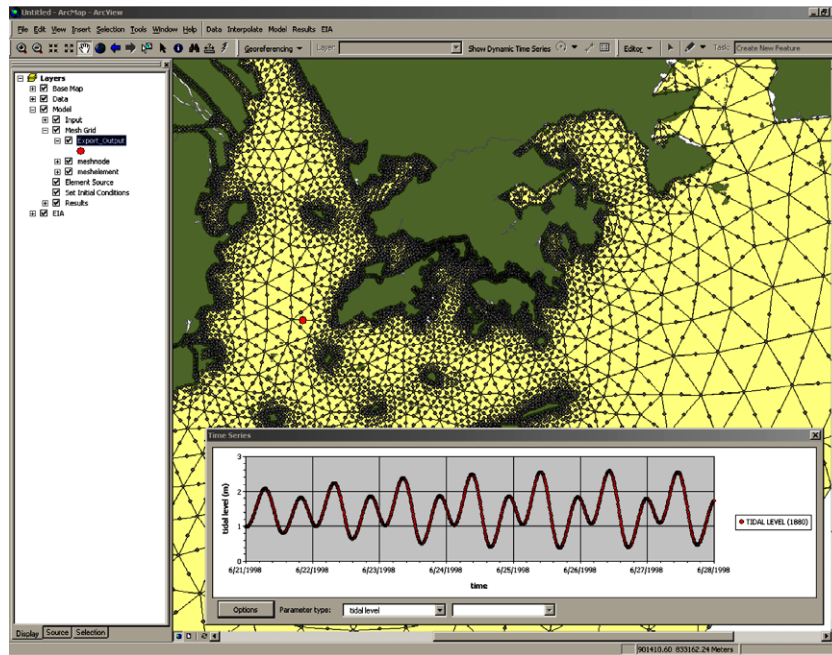


Fig. 16. Display of model output of tidal level using the GIS-model integrated system.

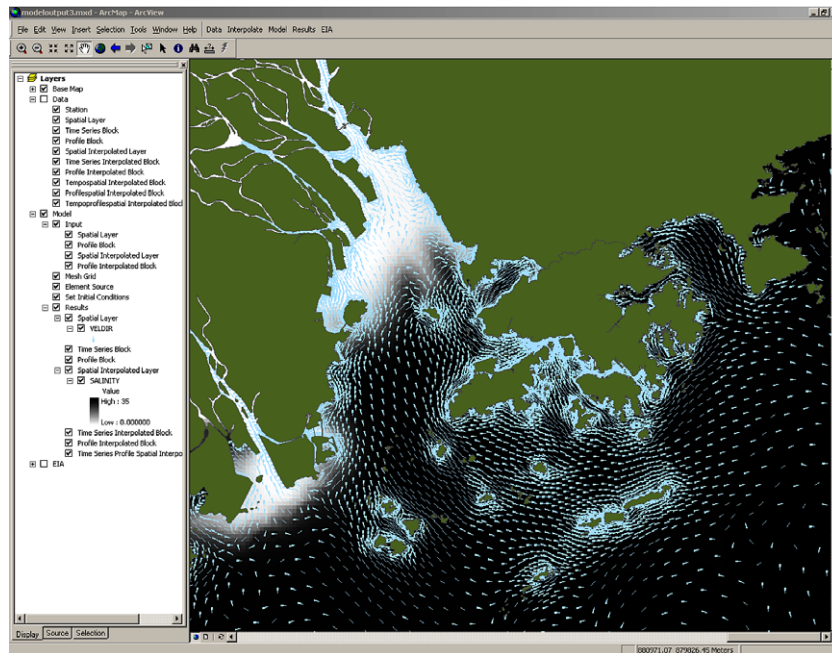


Fig. 17. Display of model outputs of current velocity and salinity for simulation time June 24, 1998 12:00:00 pm using the GIS-model integrated system.

5. Conclusions

A GIS is coupled with a complex three-dimensional hydrodynamic sediment and heavy metal transport numerical model for input viewing and editing, pre-processing, mesh grid configuration, and result interpretation. The current GIS-model integrated system marks its distinctiveness from other GIS-based hydrodynamic/pollutant transport model with its ability to facilitate three-dimensional, dynamic simulation.

The application of GIS interface in defining and interpreting model input and output information tremendously improves the

understanding of the fate and transport of pollutants, and thus promotes better decision-making in coastal environment management. The system also enhances the usage of complex three-dimensional hydrodynamic pollutant transport model through a simple and easy-to-use graphic user interface. The user-friendliness of this application thus reduces the time needed to comprehend the usage of the model particular for first-time users. Furthermore, the displaying of model output in spatial and temporal context through the GIS mapping window and the additional time series tool allows to reveal results that may be less obvious without the application of these visualization techniques in tradi-

tional analysis. Furthermore, this new visualization platform facilitates better communication of coastal water quality issues not only among environmental and engineering professionals, but also for the general public at large.

Acknowledgements

The authors acknowledge the supports provided for this work by the Hong Kong Research Grants Council (Research Grant No.: PolyU 5143/04E) and the Hong Kong Polytechnic University (Research Grant No.: G-YD93).

References

- [1] Naoum S, Tsanis IK, Fullarton M. A GIS pre-processor for pollutant transport modelling. *Environ Modell Software* 2003;20:55–68.
- [2] Tsanis IK, Boyle S. A 2D hydrodynamic/pollutant transport GIS model. *Adv Eng Software* 2001;32:353–61.
- [3] Pinho JLS, Pereira Vieira JM, Antunes do Carmo JS. Hydroinformatic environment for coastal waters hydrodynamics and water quality modelling. *Adv Eng Software* 2004;35:205–22.
- [4] Lucas A. Representation of variability in marine environmental data. In: Wright DJ, Bartlett DJ, editors. *Marine and coastal geographical information systems*. Philadelphia: Taylor & Francis; 2000.
- [5] Wai OWH, Jiang Y, Lu QM. In: Lakhan VC, editor. *Large-scale finite element modeling and parallel computation of sediment transport in coastal areas*. Amsterdam: Elsevier; 2003.
- [6] Wai OWH, Lu Q. An efficient parallel model for coastal transport process simulation. *Adv Water Resour* 2000;23:747–64.
- [7] Jiang YW. Three-dimensional numerical modelling of sediment and heavy metal transport in surface waters. PhD thesis, Department of Civil and Structural Engineering, The Hong Kong Polytechnic University, Hong Kong, China SARS; 2003.
- [8] Mellor GL, Yamada T. Development of a turbulence closure model for geophysical fluid problems. *Rev Geophys Space Phys* 1982;20(4):851–75.
- [9] Jannasch HW, Honeyman BD, Balistrieri LS, Murray JW. Kinetic of trace element uptake by marine particles. *Geochim Cosmochim Acta* 1998;52:567–77.
- [10] Shamsi UM. *GIS tools for water, wastewater, and stormwater systems*. Reston: American Society of Civil Engineer; 2002.